Plant, Cell & Environment

*Plant, Cell and Environment* (2015) doi: 10.1111/pce.12604

## Original Article

# ZmMBD101 is a DNA-binding protein that maintains Mutator elements chromatin in a repressive state in maize

Julia I. Questa[1]*, Sebastián P. Rius[1], Romina Casadevall[1] & Paula Casati[1]

[1]*Centro de Estudios Fotosintéticos y Bioquímicos (CEFOBI-CONICET), Universidad Nacional de Rosario, Suipacha 531, 2000 Rosario, Argentina*

## ABSTRACT

**In maize (*Zea mays*), as well as in other crops, transposable elements (TEs) constitute a great proportion of the genome. Chromatin modifications play a vital role in establishing transposon silencing and perpetuating the acquired repressive state. Nucleosomes associated with TEs are enriched for dimethylation of histone H3 at lysine 9 and 27 (H3K9me2 and H3K27me2, respectively), signals of repressive chromatin. Here, we describe a chromatin protein, ZmMBD101, involved in the regulation of *Mutator* (*Mu*) genes in maize. ZmMBD101 is localized to the nucleus and contains a methyl-CpG-binding domain (MBD) and a zinc finger CW (CW) domain. Transgenic lines with reduced levels of *ZmMBD101* transcript present enhanced induction of *Mu* genes when plants are irradiated with UV-B. Chromatin immunoprecipitation analysis with H3K9me2 and H3K27me2 antibodies indicated that ZmMBD101 is required to maintain the levels of these histone repressive marks at *Mu* terminal inverted repeats (TIRs) under UV-B conditions. Although *Mutator* inactivity is associated with DNA methylation, cytosine methylation at *Mu* TIRs is not affected in *ZmMBD101* deficient plants. Several plant proteins are predicted to share the simple CW-MBD domain architecture present in ZmMBD101. We hypothesize that plant CW-MBD proteins may also function to protect plant genomes from deleterious transposition.**

*Key-words*: methyl-CpG-binding domain proteins; transposon elements; UV-B.

## INTRODUCTION

Epigenetic changes involve modification of DNA activity by methylation, histone modifications or chromatin remodelling without alteration of the nucleotide sequence. In plants, one of the most common and well-characterized epigenetic phenomena is DNA methylation. In particular, methyl-CpG-binding domain (MBD) proteins usually interact with DNA when it is methylated in cytosine bases. In maize, there are 14 genes containing MBD proteins based on sequence similarity, while Arabidopsis has 13 putative MBD genes (Grafi *et al.* 2007). Out of the 13 members of the AtMBD family, eight were tested for the ability to bind methylated CpG sites, and only AtMBD5, AtMBD6 and AtMBD7 exhibited specific methyl-CpG-binding activity (Ito *et al.* 2003; Scebba *et al.* 2003; Zemach & Grafi 2003). Thus, it is not clear what the roles of the other MBDs that do not bind methylated CpG sites are.

Transposable elements (TEs) are mobile pieces of DNA that can multiply and insert themselves at new genomic positions when activated. In particular, DNA transposons encode a protein called transposase that recognizes the terminal inverted repeats (TIRs) that flank the TE, excises and then integrates the element into the new genomic site. Mobilization of TEs represents a threat to genome integrity causing chromosome breaks and rearrangements. To counteract the harmful effects of transposition, host genomes have evolved sophisticated epigenetic mechanisms. For example, *Mutator* (*Mu*) autonomous elements inactivation correlates with the methylation of their DNA sequences (Chandler & Walbot 1986; Chomet *et al.* 1987; Banks *et al.* 1988). TEs are also associated with various histone posttranslational modifications, which are characteristic of a particular repressive chromatin environment (Rigal & Mathieu 2011). Silencing of TE transcription requires H3K9me2 and H3K27me1 (Jackson *et al.* 2002; Ebbs *et al.* 2005; Ebbs & Bender 2006; Jacob *et al.* 2009). The *Mutator* family in maize consists of several elements, all sharing similar TIRs. The autonomous element *MuDR* encodes two genes, the transposase *mudrA* and a gene with unknown function *mudrB* (Eisen *et al.* 1994; Hershberger *et al.* 1995). Multiple homologous *MuDR* elements (*hMuDR*) exist in *Mutator* and non-*Mutator* maize lines (Rudenko & Walbot 2001). At the sequence level, *hMuDR* elements are highly similar to *MuDR* and share the gene structure of the autonomous element (Rudenko & Walbot 2001). Given *Mu* mutagenic potential, the host must prevent its activity. Silencing of *MuDR*/*Mu* elements is accompanied by extensive methylation (Chandler & Walbot 1986).

Transposable element reactivation occurs under different stress conditions including high temperature (Lang-Mladek *et al.* 2010; Pecinka *et al.* 2010; Tittel-Elmer *et al.* 2010), UV-B (Walbot 1999; Questa *et al.* 2013a) and pathogens (Dowen *et al.* 2012). In maize, UV-B illumination increases binding of MURA transposase to its target site within *Mutator* TIRs resulting in *Mu* elements somatic transposition (Questa *et al.* 2013a). Interestingly, we also previously found

*Correspondence: P. Casati. Fax: +54-341-4371955; e-mail: casati@cefobi-conicet.gov.ar*

**Present address: Cell and Developmental Biology, John Innes Centre, Norwich Research Park, Norwich NR4 7UH, UK*

that UV-B radiation induces the expression of *ZmMBD101,* which is in addition constitutively expressed at higher levels in maize landraces with increased UV-B tolerance (Casati *et al.* 2006). Moreover, transgenic *mbd101* RNAi maize plants were hypersensitive to UV-B (Casati *et al.* 2006) and accumulated dramatically higher levels of cyclobutane pyrimidine dimers (CPDs) after a UV-B treatment (Campi *et al.* 2012). Under normal growing conditions, the basal CPD levels in *mbd101* lines were indistinguishable from those of non-transgenic control plants, indicating a specific requirement of ZmMBD101 activity in the presence of UV-B radiation. On the other hand, transcriptome profiling revealed that a large number of transcripts increased by UV-B in *mbd101* lines suggesting a major role of ZmMBD101 in gene repression (Casati & Walbot 2008). However, the role of ZmMBD101 in maize is not clear, and there is no evidence that ZmMBD101 binds to DNA. Thus, in this work, we aimed to investigate the role of maize ZmMBD101. Here, we show that the domain architecture found in ZmMBD101 is only present in proteins belonging to the plant kingdom. ZmMBD101 exhibits a very distinct subnuclear distribution and binds to both methylated and unmethylated DNA. We also show that *mbd101* RNAi maize plants have *Mutator* elements chromatin in a less repressive state, in particular under UV-B conditions. In addition, we present evidence for a biological role of a monocot MBD protein.

## MATERIAL AND METHODS

### Plant material and radiation treatments

The *mbd101* transgenic line was previously described (Casati *et al.* 2006). Briefly, the transgenic line is in a hybrid, mainly B73 background, and contains an RNAi construct specifically directed towards *ZmMBD101* (3201-11 T-MCG3818.11; 3201-12 T-MCG3818.15; 3201-13 T-MCG3818.18; and 3201-14 T-MCG3818.19 lines). The transgene construct encodes BASTA herbicide resistance. As non-transgenic controls (CTL), siblings with the same genetic background but which lacked the transgene construct encoding BASTA herbicide resistance and the RNAi expression cassette were used. These control plants went through the transformation and regeneration process, and correspond to the T2 siblings that do not segregate the transgenes. *Mutator* active (*Mu on*) lines with *bz2-mu2* reporter alleles were used. Spotted (active) kernels from appropriate ears were selected. *B73* lines were used to address *ZmMBD101* transcript expression analysis and for western blot experiments.

Plants were grown in the greenhouse with supplemental visible light (15 h light/9 h dark) without UV-B for 28 days. UV-B was provided once for 8 h, starting 3 h after the beginning of the light period, using fixtures mounted 30 cm above the plants (Phillips, F40UVB 40 W and TL 20 W/12) at a UV-B intensity of 2 W m-2, UV-A: 0.65 W m-2. The bulbs were covered with cellulose acetate to exclude wavelengths <280 nm. As a control, plants were exposed for 8 h under the same lamps covered with polyester film (no UV-B treatment, UV-B: 0.04 W m-2, UV-A: 0.4 W m-2). Samples were collected immediately after irradiation.

*Arabidopsis thaliana* ecotype Columbia (Col-0) plants were used for subcellular localization studies. The *ddm1* T-DNA insertional mutant was described elsewhere (ddm1_093009, Questa *et al.* 2013b). Seeds were sterilized and plated on Murashige and Skoog (MS) medium supplemented with 1% (w/v) sucrose and 0.5% (w/v) Phytagel. Seeds were stratified at 4°C for 48 h and then grown in continuous light at 22°C.

### RNA isolation, reverse transcription and qPCR

Tissues from three independent biological replicates were frozen in liquid nitrogen and stored at -80°C. RNA samples were isolated using Trizol (Invitrogen) followed by DNase treatment (Promega). RNA was isolated from a pool of top leaves (which received the greatest UV-B exposure) from six plants; pooling minimizes organismal variation. A total of 5 $\mu$g of total RNA from each genotype/treatment combination was used for cDNA synthesis using Superscript II reverse transcriptase (Invitrogen) with oligo-dT as a primer. The resulting cDNAs were used as a template for qPCR amplification in a MiniOPTICON2 apparatus (Bio-Rad), using the intercalation dye SYBR Green I (Invitrogen) as a fluorescent reporter and Platinum Taq Polymerase (Invitrogen). Primers were designed to generate unique 150–250 bp-fragments using the PRIMER3 software. Three biological replicates were used for each sample plus a negative control (reaction without reverse transcriptase). To normalize the data, primers for *ACTIN1* and *THIOREDOXIN-LIKE* transcripts were used (Supporting Information Table S2). Amplification conditions were as follows: 2 min denaturation at 94°C; 40 to 45 cycles at 94°C for 10 s, 57°C for 15 s and 72°C for 20 s, followed by 5 min at 72°C. Melting curves for each PCR product were determined by measuring the decrease of fluorescence with increasing temperature (from 65°C to 95°C). To confirm the size of the PCR products and to check that they corresponded to a unique and expected PCR product, the final PCR products were separated on a 2% (w/v) agarose gel and stained with SYBR green (Invitrogen).

### Cloning, expression and purification of recombinant proteins

*ZmMBD101* cDNA was amplified using Hot Start Polymerase (Invitrogen) using the primers listed in Supporting Information Table S2, cloned into pGEX-2T and transformed into BL21 (DE3) pLys cells. The plasmid containing the GST-AtMBD5 construct was kindly provided by G. Grafi (Zemach & Grafi 2003). GST-ZmMBD101, GST-AtMBD5 and GST expression was achieved by induction of the cell culture with 0.5 mM IPTG at 37°C for 6 h. Protein purification was performed using HiTrap™ columns (GE Healthcare).

### Electrophoretic mobility shift assay

For electrophoretic mobility shift assay (EMSA) analysis, we used the double-stranded umCG oligonucleotides

 

described by (Zemach & Grafi 2003) (umCG: TCAGATT CGCGCCGGCTGCGATAAGCT). umCG oligonucleotides were methylated with *Sss*I methylase (NEB) to obtained the methylated 4mCG (4mCG: TCAGATT$^{m}$CG$^{m}$CGC$^{m}$CGGCTG$^{m}$ CGATAAGCT). Cytosine methylation was verified by restriction with *Hpa*II endonuclease. Oligonucleotides end-labelling was carried out using T4 Polynucleotide Kinase (Invitrogen) in the presence of a 2M excess of [$\gamma$-$^{32}$P]ATP (>8000 Ci/mmol). Binding reactions were performed in a buffer containing 10 mM Tris–HCl pH 7.5, 50 mM NaCl, 1mM EDTA, 5% (v/v) glycerol, 2 $\mu$g of salmon sperm DNA, 1 mM DTT with 1 ng of end-labelled, double-stranded DNA probes, for 1 h at room temperature. Protein-DNA complexes were resolved on 6% (w/v) polyacrylamide gels (30:0.8 acrylamide:bis-acrylamide) in 0.25× Tris-borate/EDTA (22.5 mM Tris-Borate and 0.5 mM EDTA) at 100 V for 90 min at 4°C.

## Generation of *Arabidopsis* transgenic plants expressing ZmMBD101-GFP

Full-length open reading frame of ZmMBD101 was amplified from complementary DNA (cDNA) obtained from leaf tissues of maize B73 lines. The primers MBD101 Fw-*Bgl*II and MBD101 Rv-*Spe*I were used for further cloning (Supporting Information Table S2). The amplified products were digested, purified and cloned into pCS052_GFP_pCHF3 (a modified version of pCHF3; GFP coding sequence without the start codon is inserted into *BamH*I and *Spe*I sites), generating Pro35S::ZmMBD101-GFP constructs.

The Pro35S::ZmMBD101-GFP construct was transformed into *Agrobacterium tumefaciens* strain GV3101 by electroporation, and the transformation of Arabidopsis plants (Col-0) was performed by the floral dip method (Clough & Bent 1998). Transformed seedlings (T1) were identified by selection on solid MS medium containing kanamycin (50 mg/L), and then the plants were transferred to soil. Expression of ZmMBD101-GFP protein in 35S::ZmMBD101-GFP lines was analysed by western blot in three independent sets of transgenic plants with positive results. Leaves from Arabidopsis seedlings were grinded and the powder was resuspended in Protein Extraction Buffer (100 mM Tris–HCl pH8, 1 mM EDTA, 10 mM MgCl2, 15 mM 2-mercaptoethanol, 20% (v/v) glycerol and 1 mM PMSF). Samples were centrifuged at 20 000 rpm during 30 min at 4°C. Total leaf extracts were loaded onto 10% (w/v) acrylamide gels and transferred to nitrocellulose membrane. Detection was performed with anti-GFP antibodies (ab290, Abcam). Bound antibody was visualized by linking to alkaline phosphatase-conjugated goat anti-mouse IgG according to the manufacturer's instructions (Bio-Rad).

## Subcellular localization analysis

Polyclonal antibodies against recombinant GST-ZmMBD101 were obtained by immunization of rabbits with 200 $\mu$g of the purified protein in four subcutaneous injections of 50 $\mu$g at 15 days intervals. The polyclonal antibodies obtained were tested by western blot with purified recombinant GST-ZmMBD101 digested with Thrombin (Calbiochem).

Nuclear proteins isolation was performed as described elsewhere (Casati *et al.* 2008). An aliquot corresponding to the cytoplasmic proteins fraction was taken in the first step of nuclear protein isolation. Fifteen and ten percent SDS-PAGE was performed with nuclear and cytoplasmic proteins, respectively. Detection was performed with the anti-GST-ZmMBD101 polyclonal antibodies generated. Bound antibody was visualized by linking to alkaline phosphatase-conjugated goat anti-rabbit IgG according to the manufacturer's instructions (Bio-Rad).

For microscopy analysis, we used seven-days-old roots from 35S::ZmMBD101-GFP Arabidopsis transgenic lines. Arabidopsis roots were used because they are relatively thin and have low background fluorescence, making them highly suitable for analysis with the epifluorescence and confocal microscope. For roots stained with propidium iodide (PI), a Zeiss 510 Meta confocal microscope was used, with an excitation line at 488 nm and detection at 580 to 700 nm. Alternatively, images of root cells and nuclei were collected with a 603 oil lens on a Nikon Eclipse 600 epifluorescence microscope equipped with a Hamamatsu Orca ER cooled CCD digital camera. The following wavelengths were used for fluorescence detection: excitation 490–510 nm and emission 520–550 nm for GFP, excitation of 340 to 380 nm and emission of 425 to 475 nm for 4′,6-diamidino-2-phenylindole (DAPI). For DAPI staining, roots were incubated in a 4 $\mu$g/mL DAPI solution during 10 min at room temperature.

## Chromatin immunoprecipitation

Chromatin immunoprecipitation (ChIP) was performed as described previously (Questa *et al.* 2010). The following antibodies were used: 4 $\mu$L of anti-H3K9me2 (ab1220), 4 $\mu$L of anti-H3K27me2 (ab6002), 4 $\mu$L of anti-H3 (ab1791) (all from Abcam); 4 $\mu$L of anti-N-terminal acetylated H3 (06-599 Upstate Biotechnology). Three biological replicates of ChIP were performed from each genotype/treatment sample type, using 3201-11 T-MCG3818.11 and 3201-12 T-MCG3818.15 transgenic lines, and three qPCR experiments were performed with each sample.

## DNA methylation analysis

The isolation of DNA templates for DNA methylation analysis by qPCR, and calculation of the percentage of methylation, was performed as previously described (Questa *et al.* 2010). Briefly, 1 $\mu$g of DNA was used for each DNA digestion reaction. Digestions were performed overnight in a volume with five units of *Sac*I or *Hin*fI, or no enzyme as a control. After digestion, each PCR template was diluted eightfold in water and incubated at 65°C to inactivate the enzyme prior to the reaction assay. Three biological replicates were performed for each sample, and three qPCR experiments were performed with each sample. The primers used for qPCR reactions are listed in Supporting Information Table S2.

### Phylogenetic analysis of CW-MBD proteins

*In silico* identification of proteins containing CW-MBD domain architecture was conducted using Conserved Domain Architecture Retrieval Tool (CDART, Geer *et al.* 2002). ZmMBD101 full length amino acid sequence was used as query. The results of the search are detailed in Supporting Information Table S1. A total of 172 protein sequences were retrieved to have the same domain architecture as ZmMBD101. Evolutionary analyses were conducted in MEGA6 (Tamura *et al.* 2013). Sequences were aligned using MUSCLE (Edgar 2004) with default settings for 1000 iterations. The evolutionary history was inferred by using the maximum likelihood method based on the Jones–Taylor–Thornton matrix-based model (Jones *et al.* 1992).

### Statistical analysis

Statistical analysis was performed using ANOVA models (Tukey test) or alternatively Student's *t* test, using untransformed data.

## RESULTS

### Analysis of ZmMBD101 structure and comparison with other plant CW-MBD proteins

Maize ZmMBD101 has two conserved chromatin-binding domains, a N-terminal CW and a C-terminal MBD domain (Fig. 1(a)). The MBD domain was originally identified in mammals (Meehan *et al.* 1989), and the sequence motif was defined by molecular analysis of the prototype protein MeCP2 (Nan *et al.* 1993). Later, it was shown that the MBD domain is found across the eukaryotic lineage (Hendrich & Tweedie 2003). The zinc finger CW (CW) domain is a zinc-binding domain comprising about 60 amino acids, named after its conserved cysteine and tryptophan residues. It was first identified in Arabidopsis as an MBD-associated domain (MAD) in a subgroup of methyl-CpG-binding proteins (Berg *et al.* 2003). The CW domain is found exclusively in vertebrates, vertebrate-infecting parasites and higher plants (Perry & Zhao 2003), and is now recognized as a type of histone recognition module (He *et al.* 2010; Hoppmann *et al.* 2011). In Arabidopsis, CW domains of EFS (also known as ASHH2/SDG8/CCR1) and the B3-containing transcriptional repressor VAL1 bind H3 peptides methylated on K4, but the preferences for the methylation state of H3K4 varies between these two proteins (Hoppmann *et al.* 2011). A conserved domains architecture analysis with CDART (Geer *et al.* 2002) using ZmMBD101 full-length protein sequence revealed the presence of the CW and MBD domains (Supporting Information Table S1) in a group of proteins all belonging to the genus Viridiplantae. Each of the domains alone is present in several proteins together with other conserved domains. However, the CW-MBD domain architecture observed in ZmMBD101 is only present in other 172 protein sequences (Supporting Information Table S1), whereas no other conserved domain seems to be present in any of these proteins. Interestingly, there is no evidence of this domain architecture outside the plant kingdom. We conclude that ZmMBD101 belongs to a subgroup of plant proteins with two major chromatin-binding domains. To date, there is no evidence of the biological role of any other member of this protein family.

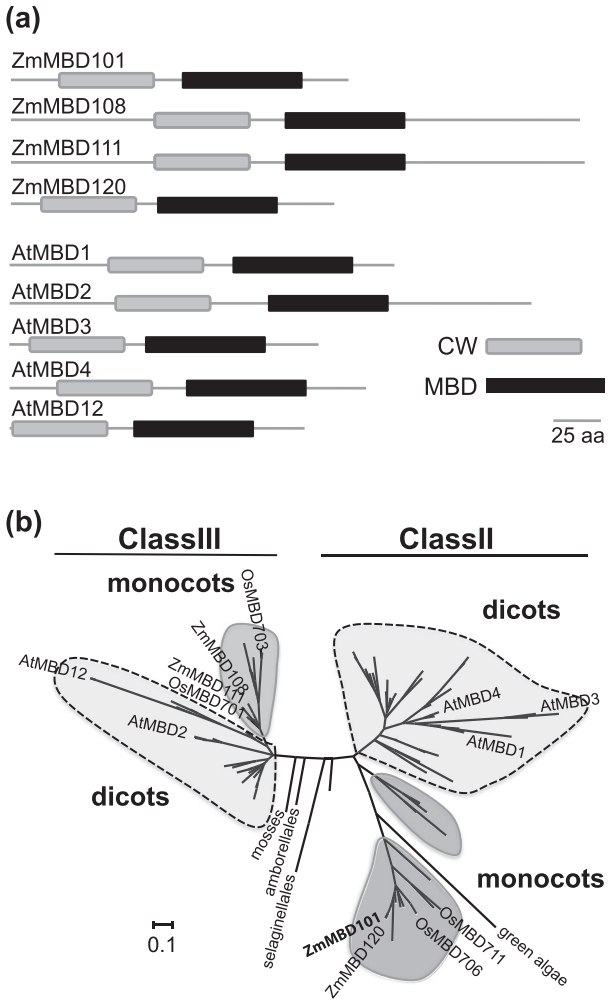


**Figure 1.** Plant CW-MBD proteins. (a) Scheme of the domain architecture of maize and *Arabidopsis* CW-MBD proteins. All these proteins share a conserved N-terminal CW and a C-terminal MBD domain. (b) Phylogenetic analysis of plant CW-MBD proteins. This analysis involved 172 amino acid sequences. The scale bar indicates the number of amino acid substitutions per site. *Arabidopsis* (At, *Arabidopsis thaliana*), maize (Zm, *Zea mays*) and rice (Os, *Oryza sativa*) members of the CW-MBD protein family are indicated. Class II and III refer to the MBD plant proteins classification previously performed by Springer and Kaeppler (2005).

Phylogenetic analysis of the CW-MBD proteins showed that the proteins clustered in two clades (Fig. 1(b)), which represent the previously classified class II and class III plant MBD proteins (Springer & Kaeppler 2005). In the latter work, the authors reported data for *Arabidopsis*, maize and rice MBD proteins. Our analysis demonstrates that the relatively simple domain architecture of maize ZmMBD101 can also be found in other monocot and dicot species, as well as in ancient plants like mosses and green algae (Fig. 1(b) and Supporting Information Table S1).

## Expression of *ZmMBD101* in maize

The pattern of expression of *ZmMBD101* was analysed in maize plants. We previously reported that *ZmMBD101* transcript is activated by UV-B, and RNAi plants with reduced levels of *ZmMBD101* showed increased sensitivity to UV-B (Casati *et al.* 2006). It has also been shown that *ZmMBD101* is expressed constitutively in different maize tissues (Springer & Kaeppler 2005). Here, we show that the expression of *ZmMBD101* is detected in both vegetative and reproductive tissues, but the expression levels vary among different parts of the plant (Fig. 2(a)). We found a peak of expression of *ZmMBD101* in leaves of 1-week old maize seedlings and a reduction of the expression levels in older leaves (Fig. 2(a)). Interestingly, we observed the same pattern in spikelets, where the expression of *ZmMBD101* is higher in immature spikelets than in pollen containing mature spikelets. However, the expression levels of *ZmMBD101* are higher in 3-week-old than in 1-week-old roots. Thus, even though *ZmMBD101* is detectable in different maize tissues, its expression levels vary during plant development.

## ZmMBD101 has DNA-binding activity

In Arabidopsis, 8 out of the 13 members of the AtMBD family were tested for their ability to bind methylated CpG sites (Zemach & Grafi 2003; Scebba *et al.* 2003; Ito *et al.* 2003). Only three of them, namely AtMBD5, AtMBD6 and AtMBD7, are referred as functional MBD proteins because they specifically bind to methylated CpG sites *in vitro*. Whereas all the other Arabidopsis proteins tested failed to bind methyl CpG sites, AtMBD4 and AtMBD11 bind both methylated and unmethylated DNA sequences (Ito *et al.* 2003; Scebba *et al.* 2003).

The biological relevance of monocot MBD proteins has yet to be investigated. The lack of evidence of the binding specificity of monocot MBD proteins prompted us to test if ZmMBD101 protein can recognize and bind 5-methylcytosine (5mCpG). To this end, we expressed and purified recombinant ZmMBD101 and AtMBD5 fused to *GLUTATHIONE S-TRANSFERASE* (GST-ZmMBD101 and GST-AtMBD5; Supporting Information Fig. S1) to perform electrophoretic mobility shift assays (EMSA). Our data indicates that GST-ZmMBD101 binds to both methylated and unmethylated double-stranded DNA (Fig. 2(b) and (c), Supporting information Fig. S2a and b). As a control, we included in our assay GST-AtMBD5 protein, which has proved capability of specifically binding methylated CpG dinucleotides (Zemach & Grafi 2003; Fig. 2(b), Supporting Information Fig. S2a) and not unmethylated DNA (Fig. 2(c), Supporting Information Fig. S2b). As expected, GST alone is not able to bind DNA in the conditions tested (Fig. 2(b) and (c)). Competition experiments verified that GST-ZmMBD101 DNA-binding ability is non-methylation specific. A hundredfold molar excess of unlabeled unmethylated competitor can reduce the formation of both methylated and unmethylated DNA-protein complexes (Supporting Information Fig. S2c and d). The ability to bind to DNA independently of the methylation status has previously been shown for AtMBD4 (Ito *et al.* 2003), which together with ZmMBD101 belongs to the Class II of plant MBD proteins (Springer & Kaeppler 2005). Moreover, it is now recognized that MeCP2 can bind to unmethylated DNA and chromatin in addition to methylated DNA (Hansen *et al.* 2010).

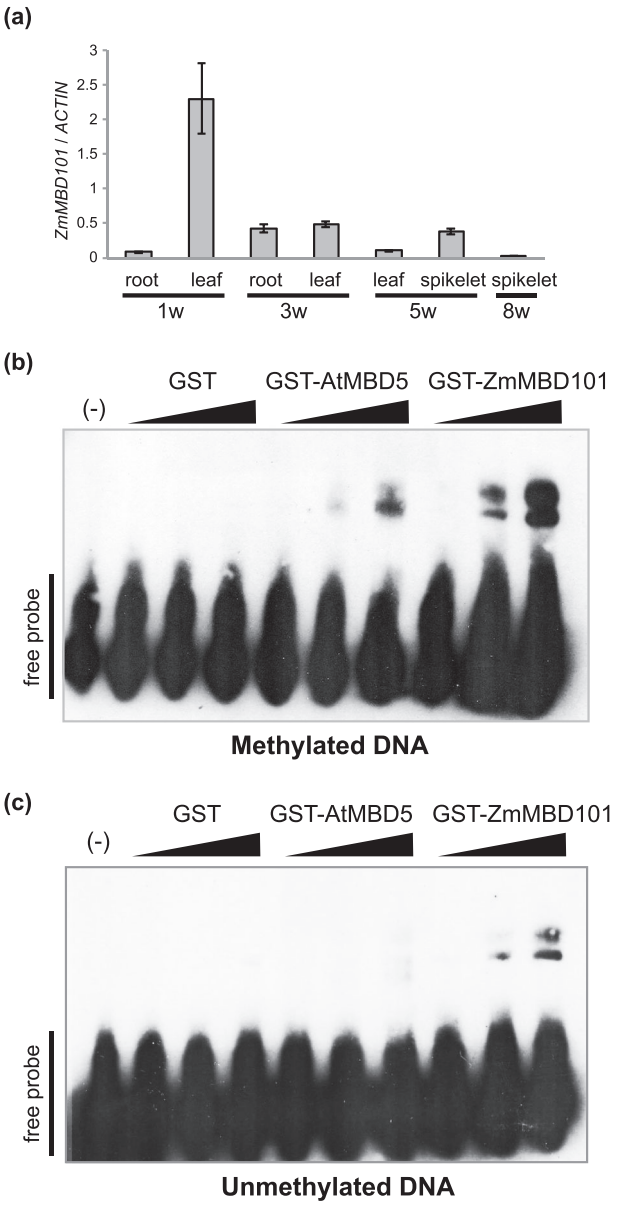


**Figure 2.** ZmMBD101 is a nuclear protein with the ability to bind DNA. (a) qRT-PCR analysis showing *ZmMBD101* transcript expression across maize development. Root, leaf and spikelet samples were collected from 1 week old (1w), 3 weeks (3w), 5 weeks (5w) and 8 weeks old B73 plants (8w). Data was normalized to *ACTIN1* transcript (GRMZM2G126010). Values are means +/− SD of three biological replicates. (b)–(c) electrophoretic mobility shift assay showing the differential binding ability of recombinant GST-ZmMBD101 and GST-AtMBD5 to (b) methylated and (c) unmethylated double stranded DNA. Increasing concentration of GST, GST-AtMBD5 and GST-ZmMBD101 (50, 125 and 250 ng of purified protein) was loaded onto the gel. (−) indicates that no protein was added to the binding reaction. For probe details see Material and Methods. Free probe is indicated at the bottom left.

## ZmMBD101 is localized to the nucleus

The predicted chromatin domains present in ZmMBD101 sequence suggest that it could be localized to the plant nuclei. However, there is no evidence that monocot MBD proteins are nuclear proteins. To analyse the subcellular localization of ZmMBD101, we raised antibodies against the recombinant GST-ZmMBD101 (Supporting Information Fig. S3a) and performed western blot analysis with maize nuclear protein extracts. We found a reactive band that corresponds to the size of ZmMBD101 (Supporting Information Fig. S3b), which is not observed in the cytosolic protein fraction (Supporting Information Fig. S3c). However, we also evidenced a second reactive band, corresponding to a higher molecular mass (Supporting Information Fig. S3b). The sequence alignment of the four maize proteins containing CW and MBD domains, ZmMBD101, ZmMBD108, ZmMBD111 and ZmMBD120, showed high sequence similarity (Supporting Information Fig. S4a). Presumably, the polyclonal antibodies generated against GST-ZmMBD101 are also reactive for the closely related proteins ZmMBD111 and ZmMBD108, with predicted molecular masses of 33.84 and 33.47 kD, respectively. ZmMBD101 has a predicted molecular mass of 20.22 kD, while ZmMBD120 has a predicted molecular mass of 19.53 kD, so it is possible that the 20 kD band could correspond to ZmMBD101, to ZmMBD120 or to both of them (Supporting Information Fig. S4b).

Thus, alternatively, to further assess the subcellular localization of ZmMBD101, we generated Arabidopsis transgenic plants that express ZmMBD101 as a fusion protein to the N-terminus of GFP driven by the cauliflower mosaic virus 35S promoter (35S::ZmMBD101-GFP lines, Supporting Information Fig. S5). Roots of 35S::ZmMBD101-GFP seedlings were inspected under a fluorescence microscope, and GFP signal indicated that ZmMBD101-GFP is exclusively localized to the nuclei (Fig. 3(a) and (b)).

## ZmMBD101-GFP presents a distinct subnuclear localization pattern

Subnuclear localization patterns were previously described for Arabidopsis MBD proteins. AtMBD5, 6 and 7 have preference for methylated CpG sites and localize to the heterochromatic chromocenters (Zemach *et al.* 2005). In contrast, AtMBD2 fails to bind to CpG sites *in vitro* and is evenly dispersed in the nuclei. We therefore investigated whether ZmMBD101-GFP presents any subnuclear pattern. Fluorescence microscopy on root cells of 35S::ZmMBD101-GFP plants revealed that ZmMBD101-GFP localizes to nucleoplasmic foci (Fig. 3(c)). Furthermore, ZmMBD101-GFP subnuclear localization does not match the DAPI-stained dense heterochromatin regions in Arabidopsis nuclei (Fig. 3(c)).

*ddm1-2*, a mutation in the SWI/SNF2 chromatin remodelling gene *DDM1* leads to a reduction in CpG methylation levels (Kakutani *et al.* 1996) and disrupts the heterochromatic localization of AtMBD5, 6 and 7 (Zemach *et al.* 2005). To test if mutations in *DDM1* gene also affect the subnuclear localization of ZmMBD101, we crossed the 35S::ZmMBD101-GFP lines to a previously reported *ddm1* T-DNA insertional mutant (ddm1_093009, Questa *et al.* 2013b). In contrast to what was observed for the Arabidopsis MBD proteins, ZmMBD101-GFP subnuclear distribution is similar in wild type (*DDM1* +/+), heterozygous (*DDM1* +/−) and homozygous (*DDM1* −/−) F2 plants (Fig. 3(d)). Together, our data shows that ZmMBD101-GFP has a very distinct subnuclear localization pattern compared with that described for the Arabidopsis counterparts. Moreover, ZmMBD101-GFP is not found in dense heterochromatin regions and its distribution remains unaffected in *ddm1* background, in agreement with its methylation independent DNA-binding activity.

## ZmMBD101 affects *Mutator* genes expression under UV-B conditions

Several lines of evidence suggest maize ZmMBD101 plays an important role in UV-B protection. We previously reported a twofold increase of *ZmMBD101* transcript after UV-B treatment (Casati *et al.* 2006). Moreover, under UV-B conditions, a noteworthy number of genes are upregulated in an *mbd101* RNAi line (Casati & Walbot 2008). The significantly higher number of transcripts increased by UV-B in this line suggests that ZmMBD101 has a major role in gene repression. To test this hypothesis, and to further characterize the role of ZmMBD101, we analysed the expression of *Mutator* genes, a well-characterized UV-B inducible system, in a ZmMBD101 RNAi transgenic background.

*Mutator* family of DNA transposons consists of autonomous *MuDR* elements, transpositionally defective *hMuDR* elements and non-autonomous *Mu* elements (Fig. 4(a)). *hMuDR* elements encode transcripts 93.5–97% identical to authentic *MuDR* elements that can be detected in both *Mutator* and non-*Mutator* maize lines (Rudenko & Walbot 2001). Using primers that do not discriminate between *MuDR* and *hMuDR*, we measured *hMUDR* transcripts levels in *ZmMBD101* deficient plants (*mbd101*) and in non-transgenic control siblings that do not segregate the transgene (*CTL*), and compared with *MuDR*/*hMuDR* transcripts levels found in *Mutator* active *bz2-mu2* lines (*Mu on*). Consistent with previous reports, *Mu on* plants present higher levels of *mudrA/hmudrA* transcripts compared with non-*Mutator* lines (Fig. 4(b)). Interestingly, the levels of *hmudrA* measured in *mbd101* plants are significantly higher than in *CTL* plants (Fig. 4(b)), depicting a possible role for ZmMBD101 in *Mutator* gene expression control. Induction of *mudrA/hmudrA* after 8 h UV-B was observed in both *mbd101* and *Mutator* active plants (Fig. 4(b)).

We then evaluated the expression of *mudrB/hmudrB*. In control conditions, the levels of *mudrB/hmudrB* transcripts are similar in *mbd101* and *Mutator* active plants, and we also observed an induction after UV-B treatment (Fig. 4(c)).

## *Mutator* chromatin is altered in *mbd101* mutants

Because TEs are potentially mutagenic, plants have evolved a set of mechanisms to recognize and silence them (reviewed in Lisch (2009)). H3K9me2 and H3K27me2 are epigenetic marks

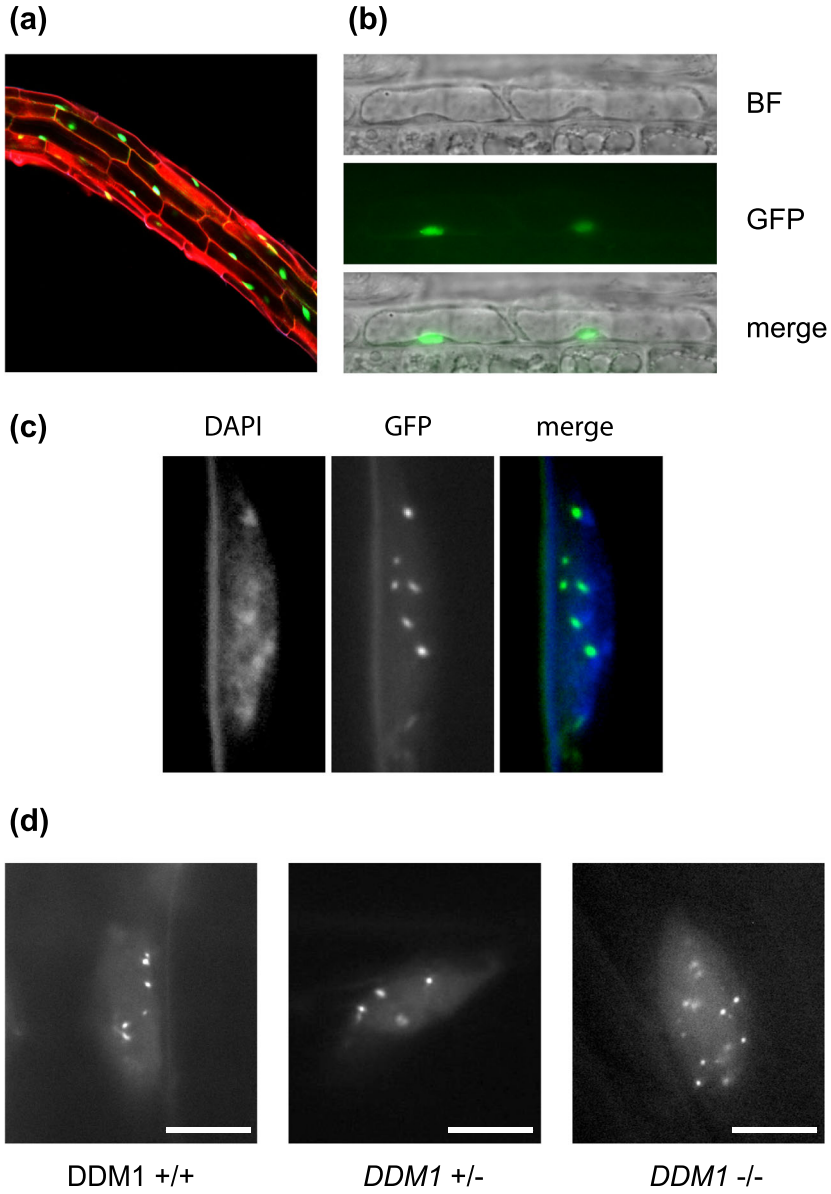


**Figure 3.** Subnuclear localization of ZmMBD101-GFP. (a) Arabidopsis root showing expression of ZmMBD101-GFP in nuclei. Seven-days-old 35S::ZmMBD101-GFP transgenic seedlings were stained with propidium iodide (PI). (b) Representative fluorescence images of root cells showing GFP signal in the nucleus. BF, brightfield. (c) Subnuclear localization of ZmMBD101GFP. Arabidopsis roots of 35S::ZmMBD101-GFP plants were stained with 4 ,6-diamidino-2-phenylindole (DAPI) and inspected under a fluorescence microscope. ZmMBD101-GFP (green) protein is localized to nucleoplasmic foci, and it is not associated with DAPI-stained heterochromatin (blue). (d) Representative images of Arabidopsis nuclei expressing ZmMBD101-GFP in wild-type and *ddm1* mutant plants. Images were taken from 7 days old wild-type (*DDM1* +/+), heterozygous (*DDM1* +/−) and homozygous (*DDM1* −/−) F2 seedlings. Bars = 5 $\mu$m.

that mediate gene silencing and are usually accompanied by DNA methylation. As for other TEs, *Mutator* transcription and transposition are subject to epigenetic control. The loss of functional *MuDR* elements leads to methylation and therefore inactivation of the non-autonomous *Mu* elements (Walbot & Rudenko 2002).

*mudrA* and *mudrB* transcripts induction by UV-B is accompanied by an increase in histone H3 acetylation and by a decrease in DNA and histone H3 methylation in *Mu1* and *MuDR* TIRs (Questa *et al.* 2010). To explore chromatin status of *Mutator* TIRs in *mbd101* plants, we analysed the accumulation of the histone repressive marks H3K9me2 and H3K27me2 by ChIP, comparing control and UV-B treated *mbd101* and non-transgenic siblings that do not segregate the transgene (*CTL*, Fig. 5(a) and (b)). Although H3K9me2 levels were slightly reduced and H3K27me2 levels were similar in *mbd101* and in the non-transgenic siblings under control conditions in the absence of UV-B (Supporting Information Fig. S6), accumulation of these repressive chromatin marks in *hMuDR* and *Mu1* TIRs was dramatically reduced by UV-B radiation in *mbd101* plants (Fig. 5(a) and (b); Supporting Information Fig. S6), suggesting that ZmMBD101 may somehow influence

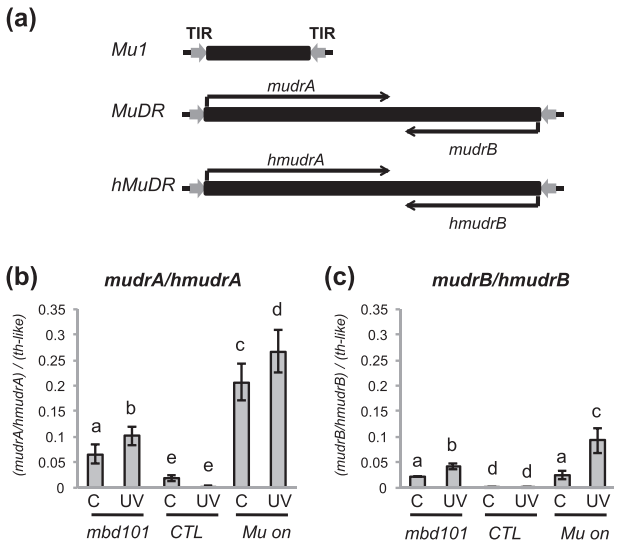


**Figure 4.** ZmMBD101 controls *Mutator* gene expression. (a) Scheme of *Mu1*, *MuDR* and *hMuDR* elements. Grey arrows indicate the conserved terminal inverted repeats (TIR). *MuDR* regulatory element encodes two genes, *mudrA* and *mudrB*. The *hMuDR* elements are organized like *MuDR*. (b)–(c) qRT-PCR analysis showing the differential expression of (b)*mudrA/hmudrA* and (c) *mudrB/hmudrB* transcripts in *mbd101* RNAi transgenic plants (*mbd101*), *Mu* active plants (*Mu on*) and non-transgenic control plants (*CTL*), in control conditions (C) and after 8 h UV-B treatment (UV). Values are means +/− SD of three biological replicates. Statistical significance was analysed using ANOVA, Tukey test with $P < 0.05$; differences from the control are marked with different letters.

H3K9me2 and H3K27me2 deposition at *Mutator* TIRs under UV-B conditions.

Histone acetylation is generally associated with active loci (Kouzarides 2007). UV-B induces the accumulation of acetylated H3 in *hMuDR* and *Mu1* TIRs in *Mutator* active and silencing plants (Questa *et al.* 2010). We analysed the enrichment of acetylated H3 caused by UV-B in *mbd101* and *CTL* plants. Surprisingly, no significant differences were observed in H3 acetylation between *mbd101* and *CTL* plants (Fig. 5(c)). As a control, immunoprecipitation was performed using antibodies against unmodified histone H3 (Fig. 5(d)). From our data we conclude that ZmMBD101 modulates *Mutator* gene activity, in particular under stress conditions, and this could be by maintaining histone repressive marks at the TIRs.

We then tested the accumulation of DNA methylation at the TIRs. We previously observed that *Mutator* activation by UV-B was accompanied by a reduction in the levels of 5mCpG at *Mu1* and *MuDR* TIRs (Questa *et al.* 2010). In the latter work, three different restriction enzymes that are sensitive to DNA methylation were used (*Sac*I, *Hpa*II and *Hinf*I). We found that the methylation status of the tested sites were significant in control plants in the absence of UV-B, while a reduction in the methylation status was mainly observed in lines in which *Mutator* was active or undergoing silencing. However, no changes in DNA methylation were detected in *CTL* lines in which the transposons had been maintained in the silenced state for many generations (Questa *et al.* 2010). Interestingly, despite the increased levels of *hmudrA* and *–B* transcripts in *mbd101* lines (Fig. 4(b) and (c)), using two of the methylation sensitive enzymes used in the experiments presented in Questa *et al.* 2010 (*Sac*I and *Hinf*I), we did not detect changes in the levels of DNA methylation at the *Mu* TIRs in the *mbd101* RNAi lines (Supporting information Fig. S7a and b). Contrarily, DNA methylation levels were as high as those observed for *CTL* plants in control conditions, and remained unaffected by UV-B treatment at both *Mu1* (Supporting Information Fig. S7a) and *hMuDR* TIRs (Supporting Information Fig. S7b). We conclude that *Mutator* transcription activation by removal of *MBD101* is not likely to be dependent on DNA methylation levels.

## DISCUSSION

In this work, we investigated the role of ZmMBD101 in gene regulation by analysing the expression of *Mutator* genes under UV-B conditions. ZmMBD101 is a maize chromatin protein that contains two well-characterized chromatin-binding domains, MBD and CW. A common feature of MBD proteins is the ability to bind to methylated CpG sites in the genome and many MBD proteins have been associated with transcriptional repression. All mammalian MBD proteins are part of histone deacetylase complexes and can be recruited to methyl CpG rich regions to repress transcription (Bird & Wolffe 1999; Ballestar & Wolffe 2001). Apart from binding methylated DNA, MeCP2 associates with Sin3a repressor complexes, NCoR and cSki (Jones *et al.* 1998; Kokura *et al.* 2001). MBD1 associates with the chromatin modifier complex Suv39h-HP1 to enhance methyl DNA mediated transcriptional repression (Fujita *et al.* 2003). ZmMBD101 exhibits some characteristics of the mammalian MBD proteins. For example, previous microarrays analysis in *mbd101* RNAi lines showed a strong requirement of MBD101 to keep an important number of genes repressed, suggesting a role of MBD101 in transcriptional repression (Casati & Walbot 2008). However, according to the results presented in this manuscript, this repressor activity is not likely to be dependent on binding to methylated CpG sites. Unlike functional *Arabidopsis* MBD proteins, ZmMBD101 binds DNA independently of the methylation status. Gel shift assay demonstrated that recombinant GST-ZmMBD101 associates with double stranded DNA sequences whereas AtMBD5-GST specifically binds methylated DNA (Fig. 2(c) and (d); Zemach & Grafi 2003). The presence of symmetric methyl-CpGs in the DNA sequence did not prevent ZmMBD101 to form DNA-protein complexes. This dual binding capacity has also been shown for MeCP2, which associates to both methylated and unmethylated regions of the genome *in vivo* (Yasui *et al.* 2007; Chahrour *et al.* 2008).

The CW domain is found in a number of chromatin-related proteins in animals and plants (Perry & Zhao 2003). The so far characterized *Arabidopsis* genes that encode CW domains are very important players in plant development. For example, EFS is a CW domain protein involved in controlling the vegetative to reproductive switch in Arabidopsis (Zhao *et al.* 2005; Yang *et al.* 2014); while

 

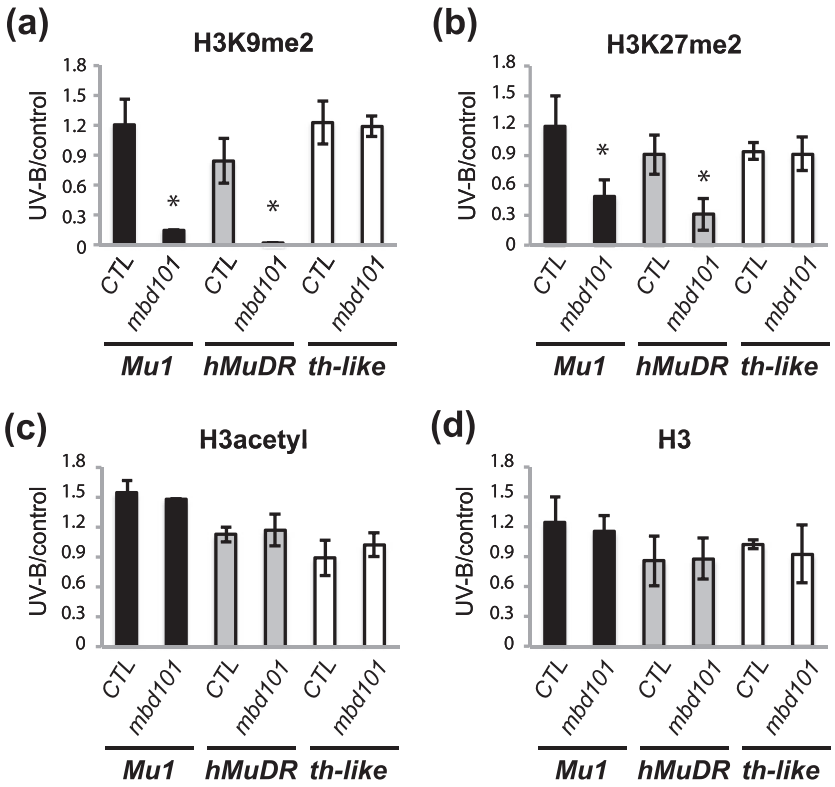


**Figure 5.** *Mutator* chromatin landscape is less repressive in *mbd101* transgenic plants under UV-B conditions. (a) Chromatin immunoprecipitation analysis of H3K9me2, (b) H3K27me2, (c) acetyl H3 and (d) total histone H3 in *mbd101*RNAi transgenic lines (*mbd101*) and in non-transgenic control lines (*CTL*), under control conditions and after 8 h UV-B treatment (UV). The immunoprecipitates were analysed for the presence of *hMuDR* and *Mu1* TIR sequences (*Mu1* and *hMuDR*, respectively), and a transcribed sequence of the control gene that is not UV-B induced *THIOREDOXIN H-TYPE* gene (GRMZM2G082886, *th-like*). Enriched fractions from UV-B treated versus control plants were compared. Values are means +/− SD of three biological replicates. Asterisks denote statistical differences applying Student's *t* test ($P < 0.05$).

VAL1, another CW domain protein, is required to repress embryonic development during vegetative growth (Suzuki *et al.* 2007). Although the CW domain was first reported to be a histone recognition module with specificity for histone H3 tails methylated on lysine 4 (He *et al.* 2010; Hoppmann *et al.* 2011), its function is somehow controversial. For example, EFS has a major H3K36 methyltransferase activity (Zhao *et al.* 2005; Yang *et al.* 2014); and the CW domain was also shown to enable the interaction of the Arabidopsis B3 transcription factor VAL2 with the HISTONE DEACETYLASE19 (HDA19; Zhou *et al.* 2013), again linking the CW domain with chromatin functions and more precisely, to gene repression.

Transposable element mobilization threatens genome stability by causing deletions, genomic rearrangements and gene miss-regulation. Given the mutagenic potential of TEs, the host imposes epigenetic silencing. *Mutator* transposon inactivation is followed by extensive DNA methylation in the TIRs of non-autonomous *Mu* (Chandler & Walbot 1986), autonomous *MuDR* (Martienssen & Baron 1994) and *hMuDR* elements (Rudenko & Walbot 2001). Although the function of *hMuDRs* remains to be elucidated, these elements produce RNA and proteins in *Mutator* and non-*Mutator* maize lines. Small RNAs of 21–26 nucleotides specific to *MuDR* and *hMuDR,* potentially involved in *Mutator* silencing, are ubiquitously present in maize. Persistently transcribed *hMuDR* could constitute a source of transposon specific small RNAs (Rudenko *et al.* 2003). However, it is to date unclear whether these elements are beneficial or not for the host. What is certainly clear is that *hMuDR* elements are subject of epigenetic silencing similarly to the active autonomous *MuDR* elements. In the present work, we show that ZmMBD101 participates in the regulation of *hMuDR* gene expression in maize.

Different biotic and abiotic stress conditions are important sources of transposon reactivation. Sessile plants growing under the sun are constantly exposed to doses of UV-B radiation. Absorption of UV-B by DNA induces the accumulation of pyrimidine photolesions (Friedberg 1995). Moreover, damage caused by UV-B can be amplified by transposon activation (Walbot 1999; Questa *et al.* 2013a). In *mbd101* transgenic lines, *MuDR/hMuDR* transcripts are enriched compared with background levels, in particular under UV-B conditions. Moreover, H3K9me2 levels at *Mu1* and *hMuDR* TIRs are strongly reduced under UV-B conditions when *ZmMBD101* is down-regulated. A minor but still significant reduction was observed for H3K27me2.

Our knowledge is very limited about how ZmMBD101 can influence H3 tails methylation status at *Mutator* chromatin. The first sensible explanation would be that ZmMBD101 binds to *Mutator* TIR DNA and either facilitates H3K9me2

methyltransferase activity or inhibits demethylase activity, and this role may be more important under stress conditions when reactivation can occur. However, ZmMBD101-GFP protein is excluded from subnuclear heterochromatic regions ruling against ZmMBD101 directly targeting TEs. Interestingly, 5mCpG levels at *Mutator* TIRs were not affected in *mbd101* plants again reinforcing that some MBD domains have other functions independent from DNA methylation. Together, our data supports the hypothesis of an indirect effect on *Mutator* chromatin instead, and future work will be required to address how this is achieved.

Proteins with ZmMBD101 domain architecture are present across the plant kingdom. It remains to be elucidated whether they also function to maintain histone repressive marks in different species. In *Arabidopsis*, several histone methyltransferases are responsible for the propagation of H3K9me2, including kryptonite/SUVH4 (KYP), SUVH5 and SUVH6, which display functional redundancy at some genomic loci. In rice, mutations in the histone H3K9 methyltransferases genes SDG714 and SDG728 also lead to TE activation (Ding *et al.* 2007; Qin *et al.* 2010). Although known in *Arabidopsis* and rice, H3K9 methyltransferases have yet to be identified in maize, and this will be necessary to test potential interactions with ZmMBD101.

Together, the experiments presented here provide the first insight into the function of plant CW-MBD proteins. Our data strongly supports that ZmMBD101, a member of the monocot CW-MBD family, is a DNA-binding protein that may have a role in repressing *Mutator* genes in maize. Several plant protein sequences were predicted to have the same domain architecture as ZmMBD101. Future analysis will be required to elucidate if CW-MBD proteins have a role in protecting genomes from deleterious effects of transposition throughout the plant kingdom.

## ACKNOWLEDGMENTS

We are very grateful to Gideon Grafi for providing the plasmid containing GST-AtMBD5 and to Stefanie Rosa for her help with image processing. This research was supported by FONCyT grants PICT 2007-711 and 2012-267 to P. C. P. C. and S. P. R. are members of the Researcher Career of the Consejo Nacional de Investigaciones Científicas y Técnicas (CONICET), and J. I. Q. and R. C. were fellows from this Institution.

## REFERENCES

Ballestar E. & Wolffe A.P. (2001) Methyl-CpG-binding proteins. Targeting specific gene repression. *European Journal of Biochemistry* **268**, 1–6.

Banks J.A., Masson P. & Fedoroff N. (1988) Molecular mechanisms in the developmental regulation of the maize suppressor-mutator transposable element. *Genes and Development* **2**, 1364–1380.

Berg A., Meza T.J., Mahic M., Thorstensen T., Kristiansen K. & Aalen R.B. (2003) Ten members of the Arabidopsis gene family encoding methyl-CpG-binding domain proteins are transcriptionally active and at least one, AtMBD11, is crucial for normal development. *Nucleic Acids Research* **31**, 5291–5304.

Bird A.P. & Wolffe A.P. (1999) Methylation-induced repression—belts, braces, and chromatin. *Cell* **99**, 451–454.

Campi M., D'Andrea L., Emiliani J. & Casati P. (2012) Participation of chromatin-remodeling proteins in the repair of ultraviolet-B-damaged DNA. *Plant Physiology* **158**, 981–995.

Casati P. & Walbot V. (2008) Maize lines expressing RNAi to chromatin remodeling factors are similarly hypersensitive to UV-B radiation but exhibit distinct transcriptome responses. *Epigenetics* **3**, 216–229.

Casati P., Stapleton A.E., Blum J.E. & Walbot V. (2006) Genome-wide analysis of high-altitude maize and gene knockdown stocks implicates chromatin remodeling proteins in response to UV-B. *The Plant Journal* **46**, 613–627.

Casati P., Campi M., Chu F., Suzuki N., Maltby D., Guan S., … Walbot V. (2008) Histone acetylation and chromatin remodeling are required for UV-B-dependent transcriptional activation of regulated genes in maize. *The Plant Cell* **20**, 827–842.

Chahrour M., Jung S.Y., Shaw C., Zhou X., Wong S.T., Qin J. & Zoghbi H.Y. (2008) MeCP2, a key contributor to neurological disease, activates and represses transcription. *Science* **320**, 1224–1229.

Chandler V.L. & Walbot V. (1986) DNA modification of a maize transposable element correlates with loss of activity. *Proceedings of the National Academy of Sciences of the United States of America* **83**, 1767–1771.

Chomet P.S., Wessler S. & Dellaporta S.L. (1987) Inactivation of the maize transposable element Activator (Ac) is associated with its DNA modification. *EMBO Journal* **6**, 295–302.

Clough S.J. & Bent A.F. (1998) Floral dip: a simplified method for Agrobacterium-mediated transformation of Arabidopsis thaliana. *The Plant Journal* **16**, 735–743.

Ding Y., Wang X., Su L., Zhai J., Cao S., Zhang D., … Cao X. (2007) SDG714, a histone H3K9 methyltransferase, is involved in Tos17 DNA methylation and transposition in rice. *The Plant Cell* **19**, 9–22.

Dowen R.H., Pelizzola M., Schmitz R.J., Lister R., Dowen J.M., Nery J.R., … Ecker J.R. (2012) Widespread dynamic DNA methylation in response to biotic stress. *Proceedings of the National Academy of Sciences of the United States of America* **109**, E2183–E2191.

Ebbs M.L. & Bender J. (2006) Locus-specific control of DNA methylation by the Arabidopsis SUVH5 histone methyltransferase. *The Plant Cell* **18**, 1166–1176.

Ebbs M.L., Bartee L. & Bender J. (2005) H3 lysine 9 methylation is maintained on a transcribed inverted repeat by combined action of SUVH6 and SUVH4 methyltransferases. *Molecular and Cellular Biology* **25**, 10507–10515.

Edgar R.C. (2004) MUSCLE: a multiple sequence alignment method with reduced time and space complexity. *BMC Bioinformatics* **5**, 113.

Eisen J.A., Benito M.I. & Walbot V. (1994) Sequence similarity of putative transposases links the maize Mutator autonomous element and a group of bacterial insertion sequences. *Nucleic Acids Research* **22**, 2634–2636.

Friedberg E.C. (1995) Out of the shadows and into the light: the emergence of DNA repair. *Trends in Biochemical Sciences* **20**, 381.

Fujita N., Watanabe S., Ichimura T., Tsuruzoe S., Shinkai Y., Tachibana M., … Nakao M. (2003) Methyl-CpG binding domain 1 (MBD1) interacts with the Suv39h1-HP1 heterochromatic complex for DNA methylation-based transcriptional repression. *Journal of Biological Chemistry* **278**, 24132–24138.

Geer L.Y., Domrachev M., Lipman D.J. & Bryant S.H. (2002) CDART: protein homology by domain architecture. *Genome Research* **12**, 1619–1623.

Grafi G., Zemach A. & Pitto L. (2007) Methyl-CpG-binding domain (MBD) proteins in plants. *Biochimica et Biophysica Acta* **1769**, 287–294.

Hansen J.C., Ghosh R.P. & Woodcock C.L. (2010) Binding of the Rett syndrome protein, MeCP2, to methylated and unmethylated DNA and chromatin. *IUBMB Life* **62**, 732–738.

He F., Umehara T., Saito K., Harada T., Watanabe S., Yabuki T., … Muto Y. (2010) Structural insight into the zinc finger CW domain as a histone modification reader. *Structure* **18**, 1127–1139.

Hendrich B. & Tweedie S. (2003) The methyl-CpG binding domain and the evolving role of DNA methylation in animals. *Trends in Genetics* **19**, 269–277.

Hershberger R.J., Benito M.I., Hardeman K.J., Warren C., Chandler V.L. & Walbot V. (1995) Characterization of the major transcripts encoded by the regulatory MuDR transposable element of maize. *Genetics* **140**, 1087–1098.

Hoppmann V., Thorstensen T., Kristiansen P.E., Veiseth S.V., Rahman M.A., Finne K., … Aasland R. (2011) The CW domain, a new histone recognition module in chromatin proteins. *EMBO Journal* **30**, 1939–1952.

Ito M., Koike A., Koizumi N. & Sano H. (2003) Methylated DNA-binding proteins from Arabidopsis. *Plant Physiology* **133**, 1747–1754.

Jackson J.P., Lindroth A.M., Cao X. & Jacobsen S.E. (2002) Control of CpNpG DNA methylation by the KRYPTONITE histone H3 methyltransferase. *Nature*, **416**, 556–560.

Jacob Y., Feng S., LeBlanc C.A., Bernatavichute Y.V., Stroud H., Cokus S., … Michaels S.D. (2009) ATXR5 and ATXR6 are H3K27 monomethyltransferases

 

required for chromatin structure and gene silencing. *Nature Structural and Molecular Biology* **16**, 763–768.
Jones D.T., Taylor W.R. & Thornton J.M. (1992) The rapid generation of mutation data matrices from protein sequences. *Computer Applications in the Biosciences* **8**, 275–282.
Jones P.L., Veenstra G.J., Wade P.A., Vermaak D., Kass S.U., Landsberger N., … Wolffe A.P. (1998) Methylated DNA and MeCP2 recruit histone deacetylase to repress transcription. *Nature Genetics* **19**, 187–191.
Kakutani T., Jeddeloh J.A., Flowers S.K., Munakata K. & Richards E.J. (1996) Developmental abnormalities and epimutations associated with DNA hypomethylation mutations. *Proceedings of the National Academy of Sciences of the United States of America* **93**, 12406–12411.
Kokura K., Kaul S.C., Wadhwa R., Nomura T., Khan M.M., Shinagawa T., … Ishii S. (2001) The Ski protein family is required for MeCP2-mediated transcriptional repression. *Journal of Biological Chemistry* **276**, 34115–34121.
Kouzarides T. (2007) Chromatin modifications and their function. *Cell* **128**, 693–705.
Lang-Mladek C., Popova O., Kiok K., Berlinger M., Rakic B., Aufsatz W., … Luschnig C. (2010) Transgenerational inheritance and resetting of stress-induced loss of epigenetic gene silencing in Arabidopsis. *Molecular Plant* **3**, 594–602.
Lisch D. (2009) Epigenetic regulation of transposable elements in plants. *Annual Review of Plant Biology* **60**, 43–66.
Martienssen R. & Baron A. (1994) Coordinate suppression of mutations caused by Robertson's mutator transposons in maize. *Genetics* **136**, 1157–1170.
Meehan R.R., Lewis J.D., McKay S., Kleiner E.L. & Bird A.P. (1989) Identification of a mammalian protein that binds specifically to DNA containing methylated CpGs. *Cell* **58**, 499–507.
Nan X., Meehan R.R. & Bird A. (1993) Dissection of the methyl-CpG binding domain from the chromosomal protein MeCP2. *Nucleic Acids Research* **21**, 4886–4892.
Pecinka A., Dinh H.Q., Baubec T., Rosa M., Lettner N. & Mittelsten Scheid O. (2010) Epigenetic regulation of repetitive elements is attenuated by prolonged heat stress in Arabidopsis. *The Plant Cell* **22**, 3118–3129.
Perry J. & Zhao Y. (2003) The CW domain, a structural module shared amongst vertebrates, vertebrate-infecting parasites and higher plants. *Trends in Biochemical Sciences* **28**, 576–580.
Qin F.J., Sun Q.W., Huang L.M., Chen X.S. & Zhou D.X. (2010) Rice SUVH histone methyltransferase genes display specific functions in chromatin modification and retrotransposon repression. *Molecular Plant* **3**, 773–782.
Questa J.I., Walbot V. & Casati P. (2010) Mutator transposon activation after UV-B involves chromatin remodeling. *Epigenetics* **5**, 352–363.
Questa J., Walbot V. & Casati P. (2013a) UV-B radiation induces Mu element somatic transposition in maize. *Molecular Plant* **6**, 2004–2007.
Questa J.I., Fina J.P. & Casati P. (2013b) DDM1 and ROS1 have a role in UV-B induced- and oxidative DNA damage in A. thaliana. *Frontiers in Plant Science* **4**, 420.
Rigal M. & Mathieu O. (2011) A "mille-feuille" of silencing: epigenetic control of transposable elements. *Biochimica et Biophysica Acta* **1809**, 452–458.
Rudenko G.N. & Walbot V. (2001) Expression and post-transcriptional regulation of maize transposable element MuDR and its derivatives. *The Plant Cell* **13**, 553–570.
Rudenko G.N., Ono A. & Walbot V. (2003) Initiation of silencing of maize MuDR/Mu transposable elements. *The Plant Journal* **33**, 1013–1025.
Scebba F., Bernacchia G., De Bastiani M., Evangelista M., Cantoni R.M., Cella R., … Pitto L. (2003) Arabidopsis MBD proteins show different binding specificities and nuclear localization. *Plant Molecular Biology* **53**, 715–731.
Springer N.M. & Kaeppler S.M. (2005) Evolutionary divergence of monocot and dicot methyl-CpG-binding domain proteins. *Plant Physiology* **138**, 92–104.
Suzuki M., Wang H.H. & McCarty D.R. (2007) Repression of the LEAFY COTYLEDON 1/B3 regulatory network in plant embryo development by VP1/ABSCISIC ACID INSENSITIVE 3-LIKE B3 genes. *Plant Physiology* **143**, 902–911.
Tamura K., Stecher G., Peterson D., Filipski A. & Kumar S. (2013) MEGA6: Molecular Evolutionary Genetics Analysis version 6.0. *Molecular Biology and Evolution* **30**, 2725–2729.
Tittel-Elmer M., Bucher E., Broger L., Mathieu O., Paszkowski J. & Vaillant I. (2010) Stress-induced activation of heterochromatic transcription. *PLoS Genetics*, **6**, e1001175.
Walbot V. (1999) UV-B damage amplified by transposons in maize. *Nature*, **397**, 398-399.
Walbot V. & Rudenko G.N. (2002) MuDR/Mu transposons of maize. In *Mobile DNA II* (eds N.L. Craig, R. Craigie, M. Gellert & A. Lambowitz) pp. 533–564. Amer. Soc. Microbiology, Washington, D. C.
Yang H., Howard M. & Dean C. (2014) Antagonistic roles for H3K36me3 and H3K27me3 in the cold-induced epigenetic switch at Arabidopsis FLC. *Current Biology* **24**, 1793–1797.
Yasui D.H., Peddada S., Bieda M.C., Vallero R.O., Hogart A., Nagarajan R.P., … Lasalle J.M. (2007) Integrated epigenomic analyses of neuronal MeCP2 reveal a role for long-range interaction with active genes. *Proceedings of the National Academy of Sciences of the United States of America*, **104**, 19416–19421.
Zemach A. & Grafi G. (2003) Characterization of Arabidopsis thaliana methyl-CpG-binding domain (MBD) proteins. *The Plant Journal*, **34**, 565-572.
Zemach A., Li Y., Wayburn B., Ben-Meir H., Kiss V., Avivi Y., … Grafi G. (2005) DDM1 binds Arabidopsis methyl-CpG binding domain proteins and affects their subnuclear localization. *The Plant Cell* **17**, 1549–1558.
Zhao Z., Yu Y., Meyer D., Wu C. & Shen W.H. (2005) Prevention of early flowering by expression of FLOWERING LOCUS C requires methylation of histone H3 K36. *Nature Cell Biology* **7**, 1256–1260.
Zhou Y., Tan B., Luo M., Li Y., Liu C., Chen C., . . . Huang S. (2013) HISTONE DEACETYLASE19 interacts with HSL1 and participates in the repression of seed maturation genes in Arabidopsis seedlings. *The Plant Cell*, **25**, 134-148.

*Received 27 January 2015; received in revised form 25 June 2015; accepted for publication 26 June 2015*

## SUPPORTING INFORMATION

Additional supporting information may be found in the online version of this article at the publisher's web-site:

**Table S1.** List of protein sequences retrieved by CDART analysis.
**Table S2.** List of primers.
**Figure S1.** Purification of GST-fused recombinant proteins. Protein purification was performed using HiTrapTM columns (GE Healthcare).
**Figure S2.** EMSA showing the differential binding ability of recombinant GST-ZmMBD101 and GST-AtMBD5 to methylated (a) and unmethylated (b) double stranded DNA.
**Figure S3.** (a) Western blot analysis to test the polyclonal antibodies generated against recombinant GST-ZmMBD101 (a-MBD101).
**Figure S4.** (a) Alignment of the four maize CW-MBD proteins. Full length aminoacid sequences were aligned with MUSCLE (MEGA6).
**Figure S5.** Expression of ZmMBD101-GFP in Arabidopsis transgenic lines.
**Figure S6.** Mutator chromatin landscape is less repressive in mbd101 transgenic plants under UV-B conditions. ChIP analysis of H3K9me2 (A), H3K27me2 (B), acetyl H3 (C) and total histone H3 (D) in mbd101 RNAi transgenic lines (mbd101) and in non-transgenic control lines (CTL), under control conditions and after 8h UV-B treatment.
**Figure S7.** DNA methylation at Mutator TIRs is not affected in mbd101plants. qPCR analysis from digested DNA from mbd101RNAi transgenic and non-transgenic control (CTL) plants under control conditions (C) and after 8h UV-B treatment (UV).